

# Graphene nano scrolls responding to superlow friction of amorphous carbon



Zhenbin Gong<sup>a, b</sup>, Jing Shi<sup>a, b</sup>, Bin Zhang<sup>a</sup>, Junyan Zhang<sup>a, \*</sup>

<sup>a</sup> State Key Laboratory of Solid Lubrication, Lanzhou Institute of Chemical Physics, Chinese Academy of Sciences, Lanzhou 730000, China

<sup>b</sup> University of Chinese Academy of Sciences, Beijing, 10049, China

## ARTICLE INFO

### Article history:

Received 4 November 2016

Received in revised form

25 January 2017

Accepted 31 January 2017

Available online 1 February 2017

## ABSTRACT

Amorphous carbon films are widely used as solid lubricant coating. However, the mechanism response for its superlow friction has not been well explored. The previous results indicated that graphitic tribofilms are formed at rubbing interfaces, which leading to decreasing of friction coefficient. But in some cases, the friction coefficients of graphite (0.1–0.6) are much high than the amorphous carbon films (0.05–0.01), where the graphitic theory is quite limited and the interpretation is poor. Using high resolution transmission electron microscopy and Raman spectra, we monitor the structure evolution of tribofilms and friction coefficient drop during running-in. We demonstrate that a kind of graphene nano scroll particle was developed in the tribofilms consisting of outer graphene shell and inner amorphous core. And the relationship between friction drop and graphene nano scroll evolution suggests that, incommensurate contact of such nano scrolls, may be the dominant dissipation modes for amorphous carbon.

© 2017 Elsevier Ltd. All rights reserved.

## 1. Introduction

Amorphous carbon (a-C) film is one of the most promising solid lubricant coating in various tribological applications, for it can considerably reduce friction and wear, and extend lifetime of moving parts [1–3]. Common wisdom holds that low friction of a-C film is attributed to shear induced tribofilm formation at rubbing interfaces [4], whereas the soft graphitic tribofilms with low shear resistance, which ensure the easy slippage and lead to the friction decreasing to low value [5,6]. Generally, the a-C is metastable amorphous material composed of  $sp^3$  and  $sp^2$  bonds, and the  $sp^3$  bonds embedded in the amorphous evolves to  $sp^2$  bonds during friction and form a graphitic tribofilm [7,8]. Molecular dynamics simulations also confirmed the above  $sp^3$ -to- $sp^2$  graphitic transformation [9]. Thus, the formation of such graphitic layers was considered to be an important reason for superlow friction of a-C [7–9]. Since, under incommensurate contact, the friction coefficient of carefully prepared C-plane of HOPG is as low as  $7 \times 10^{-5}$ , which is known as “superlubricity” [10–12]. However, similar to friction induced graphitic structures [7], general graphite materials are multi-crystal and the coefficient of friction varies from 0.1 to 0.6

[13]. According to these results, it will be self-supported that the coefficient of a-C can be as low as that of graphite. However, in some cases, a-C had been proved to be with superlow frictional behavior, and the friction coefficient can be below 0.05,<sup>14</sup> which is much lower than graphite ( $\mu > 0.1$ ) [13]. This phenomenon hints that the superlow friction is related to graphitic transformation but not limited to this, since the  $sp^2$  carbon has many allotropes with diverse structures and friction properties.

For many a-C surfaces with superlow friction, the superlow friction was proved not to present immediately at sliding start but after two common stages [1–6]. First, a high friction coefficient ( $>0.1$ ) emerges, then it decreases to low or superlow friction ( $<0.05$ ) and tends to be stable [14]. These two stages of friction coefficient evolution processes are called running-in. Time of flight secondary ion mass spectrometry (TOF-SIMS) studies demonstrated that the initial a-C surfaces are covered by oxygen rich layers when exposed to air [15]. At the start of friction, the contaminant surfaces are removed by shear force, and the contact surface of a-C detaches, reacts, and transfers to the counterface [16]. During this stage, the surface presents a higher friction because of the above interfacial actions. Then the amorphous structure begins to evolve to the graphite structure, and a thick graphitic tribofilm formed on the counter surface [4,5], accompanied with friction coefficient decrease. Hence, the running-in has a very important significance for understanding the origin of the low friction of a-C,

\* Corresponding author.

E-mail address: [zhangjunyan@licp.cas.cn](mailto:zhangjunyan@licp.cas.cn) (J. Zhang).

and here we design an experiment to investigate structure evolution in running-in to reveal the underlying physical mechanism.

In this paper, we studied the nanostructure evolution of tribofilm to probe the running-in of a-C film. High resolution transmission electron microscopy (HRTEM), Raman spectrum and friction experiments demonstrate that unique graphene nano scrolls (GNSs) with outer graphene shell and inner amorphous core formed in the tribofilm. The growth of such nanoscrolls in tribofilm accompanied with the decrease of friction coefficient, which suggests that the evolution from a-C to GNSs is responding to the friction drop during running-in. Consequently, the evolution of GNSs indicates that incommensurate and rolling contact within the friction interface may be the dominant dissipation modes for amorphous carbon. The evolution path of GNSs was divided into two stages: 1) amorphous to graphene, 2) graphene to nanoscroll, which probably responds to the physical origin of superlow friction of a-C films.

## 2. Experimental

### 2.1. Sample preparation

The hydrogenated a-C films used in this study were synthesized by plasma enhanced chemical vapor deposition technique (PECVD) using a negative voltage of  $-800$  V to a substrate and a chamber pressure of  $\sim 20$  Pa. The source gases used for deposition were  $\text{CH}_4$  and  $\text{H}_2$  with a flow rate of 1:2. And the thickness of a-C films were controlled about 1000 nm. For nanostructure analysis, the HRTEM samples were grown on freshly cleaved NaCl wafers with a thickness about 20 nm. Then the NaCl wafers were placed into the deionized water, using micro grid picked up the floating a-C fragment. The HRTEM samples of tribofilms were prepared using micro grid polishing the fragments of tribofilms surfaces from the sliding balls after friction tests.

### 2.2. Structure characterizations

The nanostructures of a-C films and wear debris were analyzed on HRTEM JEM 3010(JEOL, JP) and Tecnai-G2 F20 (FEI, US). In addition to HRTEM, further information regarding the structural arrangement, chemical state and chemical bond were studied from micro Raman spectrometer (LABRAM HR 800 at a wavelength of 532 nm (2.3eV)) and X-ray photoelectron spectroscopy (XPS, ESCALAB 250XI equipped with a monochromatic X-ray source), respectively.

### 2.3. Mechanical characterization

The mechanical properties of as prepared a-C films were measured by nanoindentation (Hysitron Ti-950) with a trigonal Berkovich diamond tip. The elastic recovery  $R$  is obtained by calculation ( $R = d_{\text{max}} - d_{\text{res}} / d_{\text{max}} \times 100\%$ ), where  $d_{\text{max}}$  and  $d_{\text{res}}$  are the maximum and residual displacement.

### 2.4. Friction and wear characterization

A rotating ball-on-disk tribometer was used to measure friction coefficient by dual balls from  $\text{Al}_2\text{O}_3$ ,  $\text{Si}_3\text{N}_4$ ,  $\text{ZrO}_2$  and steel with a diameter of 5 mm. The applied load spans from 2N to 20N, under the frequency of 500r/min with a rotating radius of 4 mm. The test condition is atmospheric with a humidity about 20% and the temperature is 20 °C. After friction test, the wear of the substrate and tribofilms on the balls were imaged by optical microscope using Olympus BX53 (Olympus, Tokyo, Japan) with a magnification ten.

## 3. Results and discussions

As mentioned in the instruction section that running-in might depend on the tribofilm structure, therefore, to characterize the structure of carbon film is the first step so as to probe the nanostructure evolution of tribofilm. The a-C films for the friction test are prepared by the PECVD method using the Si (100) as the substrate (Fig. 1a). HRTEM image (Fig. 1b) presents that the as-prepared carbon films show a typical amorphous structure without any ordered structure. The inset selected area electron diffraction (SEAD) image also illustrates that the amorphous nature of so-made a-C film, in which no diffusing ring can be observed. And the fine bonding structures in the amorphous network were analyzed from their Raman spectra, shown in Fig. 1c with two bands at  $1332\text{ cm}^{-1}$  and  $1532\text{ cm}^{-1}$ , corresponding to the D and G modes of a-C, respectively [17]. XPS is used to investigate the chemical nature of the amorphous carbon network (Fig. 1d). The  $\text{C}_{1s}$  spectrum indicates a max intensity located at 284.8eV, which presents the composite structure of  $\text{sp}^3$  and  $\text{sp}^2$  bonds [18].

The mechanical properties of carbon film have a decisive influence on their friction properties [1]. Table 1 summarized the mechanical property parameters of the a-C film from their nano-indentation test, which indicate a hardness of 11.4 GPa, elastic module of 90.2 GPa and elastic recovery about 77%.

Friction behaviors of specimens were evaluated by the ball-on-disk rotating method (Fig. 2a). A typical running-in process (Fig. 2b) can be observed from their friction curves, with an initially maximum friction of 0.16 decreased slowly to a finally stable value of 0.016 after about 2000 cycles. Induced by stress, the surfaces of the counterparts transformed, and tribofilms different from sliding balls and a-C films were formed. Fig. 2c shows the morphology of new surfaces of counterpart  $\text{Al}_2\text{O}_3$  balls (top) and a-C surfaces (bottom) at different stages of running-in. Tribofilms were rapidly developed on the balls with the evolution of friction. The width of the wear track on a-C films and balls increased gradually along with the wear debris accumulated. While, accompanied with friction surface evolution, the atoms of tribofilms rearrangement and form graphitic layers [5–8]. But the specific structure type, evolution process, and lubricity mechanism of such graphitic layers are not yet clear. These questions will be investigated in detail in the following aspects: 1) the nanostructure of the tribofilms, 2) the elemental composition of tribofilms, 3) and the physical original of superlow friction.

Fig. 3a shows a series of Raman spectra of the tribofilms at different sliding cycles, corresponding to those in Fig. 2c. Remarkably, with increased friction cycles, the D and G mode were separated gradually and shift to high wave number. In this conversion process, amorphous carbon transform into a graphitic structure [19–21]. For more details, these Raman spectra were decomposed by Gauss module. Generally, the D peak and G peak can be discussed separately. The D peak strength is proportional to the probability of finding a six-fold ring in the cluster [22]. And, the G peak relates only to bond stretching of  $\text{sp}^2$  pairs [22]. Fig. 3b presents additional information of the peak shift and the  $I_D/I_G$  values. Both the D and G peak moved to high wave number, and the  $I_D/I_G$  value increased accordingly. In amorphous carbon, the increase of  $I_D/I_G$  value implies an improvement in the degree of order [23]. At the same time, the full width at half maximum (FWHM) can value the crystallinity of materials. The increase in the degree of order was also convinced by G peak's FWHM (Fig. 3c), which confirmed the structure evolution from amorphous to graphitic structure [23]. These results indicate that a large number of ordered graphitic structure are generated in the tribofilm during friction, where an interface self organizing process may occurred.

The friction behavior and lubricity mechanism of tribofilm

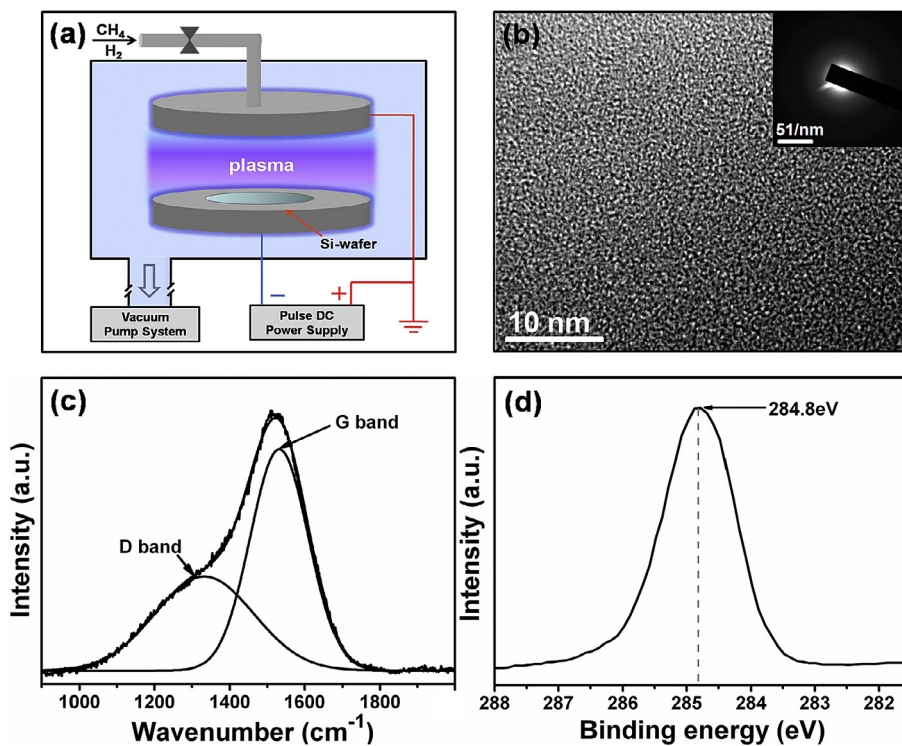


**Fig. 1.** (a) Model of the plasma-enhanced chemical vapor deposition (PECVD) technique. (b) High resolution transmission electron micrographs and electron diffraction pattern, and the selected area electron diffraction (SEAD) image. (c) Raman spectra and corresponding Gauss decomposition. (d) XPS  $C_{1s}$  spectra of a-C: films spectra. (A colour version of this figure can be viewed online.)

**Table 1**  
Mechanical properties of a-C film.

	Indentation depth nm	Hardness GPa	Elastic module GPa	Elastic recovery %
Value	98	11.4	90.2	77%

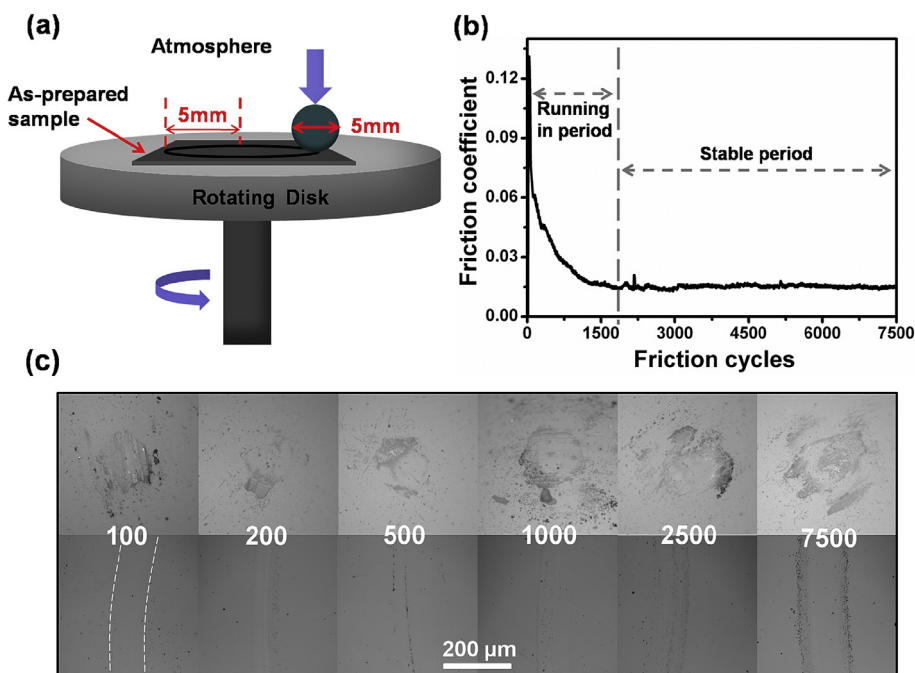


**Fig. 2.** (a) The schematic diagram of friction test machine with ball-on disk rotating mode. (b) Frictional curve of carbon films in the air with 20% humidity: the friction coefficient as a function of friction cycles. (c) The micrographs of  $Al_2O_3$  balls (top images) and a-C surfaces (bottom images) at 100, 200, 500, 1000, 2500, 7500 friction cycles, respectively. (A colour version of this figure can be viewed online.)

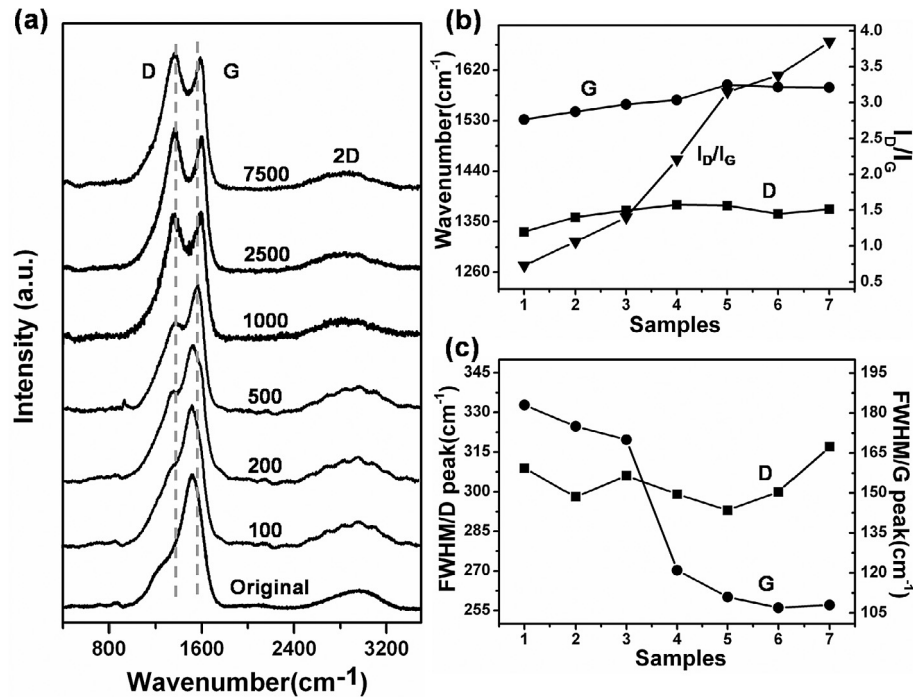


**Fig. 3.** (a) Raman spectra of tribofilms at different cycles, respectively. (b) G and D band position measured at 532 nm, and  $I_D/I_G$  of tribofilms at 0–7500 friction cycles. (c) The FWHM of D and G band.

depend on the element composition and nanostructure. Thus, the detailed atoms configuration and reconfiguration (during running-in) were studied on their HRTEM images [24]. Fig. 4 shows the HRTEM images of the tribofilm debris that unique GNSs were observed in the tribofilm (Fig. 4a). The elements and structures have been studied more comprehensively based on HRTEM and Electronic Differential System (EDS). Fig. 4b indicates that the graphene are coiled into annular or tubular form, and the graphene encapsulated on an amorphous core, which comprise the majority of tribofilm. The images show GNSs core-shell structure particle which were observed on HRTEM of the bright and dark field mode (Fig. 4b and c, insert line marks the scan range, the scanning direction is from left to right). From the C, O, Al EDS map (Fig. 4d), it can be concluded that the GNSs are mainly composed of carbon without counterpart elements. The HRTEM and EDS clearly demonstrated a core-shell structure of amorphous carbon coated with graphene (GNSs). Molecular dynamics simulations indicate that the formation of GNSs are a self-sustained curling process after a critical overlap area is reached, since the scroll formation has a lower energy than the precursor graphene [25]. In fact, the graphene sheets can generate scrolls to reducing the energy during friction, and when in the presence of cores this transformation becomes easier [26,27]. Therefore, for a-C films, the friction induced graphene layers can hardly maintain its flat structure, and will coiled into a scroll structure, which could be a common characteristic of carbon films.

Our experimental studies also confirmed that the GNSs formation occurs over a wide range of test conditions; i.e., when the substrate changed to Si<sub>3</sub>N<sub>4</sub>, Steel or ZrO<sub>2</sub>, load was changed from 2N to 20N, sliding speed was varied from 1.5m/min to 9.5 m/min, and humidity from 20% to 45%. For example, the HRTEM images of the tribofilm debris under different duality (Fig. 5) of Al<sub>2</sub>O<sub>3</sub>, Si<sub>3</sub>N<sub>4</sub>, Steel or ZrO<sub>2</sub> and load (Fig. 6) at 2N, 5N, 10N and 20N, respectively. Our results suggest that a large number of GNSs are generated in the debris, which is independent of the duality materials and test

parameters. These findings suggest that the formation of GNSs is a common phenomenon in the friction process of a-C films.

In order to reveal the mechanism for friction drop during running-in, it is necessary to correlate a certain structural feature with friction coefficient during amorphous-to-GNS transformation. Accordingly, the running-in was divided into several stages to monitor the structure evolvement and friction evolution. At the first 100 cycles (Fig. 7a), the tribofilm debris show a typical amorphous structure, but some graphene layers can be observed (Fig. 7a), which indicates that the structure evolution is quick and immediate [6]. Therefore, the friction coefficient dropped from 0.16 to 0.068 is related to the evolution of the graphitic hybridization, which is supported by previous experiments [4]. Surprisingly, just after 200 cycles, the graphene layers (Fig. 7b) introduce some new feature that the graphene begin to bend to form a graphene nanoscroll. Within a minute (500 cycles), a large amount of GNSs have been observed in the debris (Fig. 7c) and the friction coefficient declined to 0.038. And, after 1000 cycles, the GNSs become more regular and tend to be a ring structure but mixed with flat graphene sheets (Fig. 7d). When the friction coefficient reaches a stable value at 0.015 after 2500 cycles, the GNSs exhibit a more regular structure (Fig. 7e and f). It can be seen, after the running in, the friction couple reached equilibrium state and the nanoparticles exist in tribofilm debris with few graphene without curl. The electron diffraction (ED) also confirmed that with the increase of friction cycles sharper rings can be observed, indicating a more ordered structure. Generally speaking, for a-C films, a substantial amount of GNSs formed in the wear track led to the decrease of friction (see Table 2).

Further study of the GNS evolution path, can afford a deeper understanding of friction mechanism during the running-in. The formation process of such GNSs can be divided into three stages: 1) periodic shear stress and friction heating induced the formation of graphene sheets [28]; 2) the edge of graphene sheets are highly reactive and easily attach to the dangling bonds on the surface of

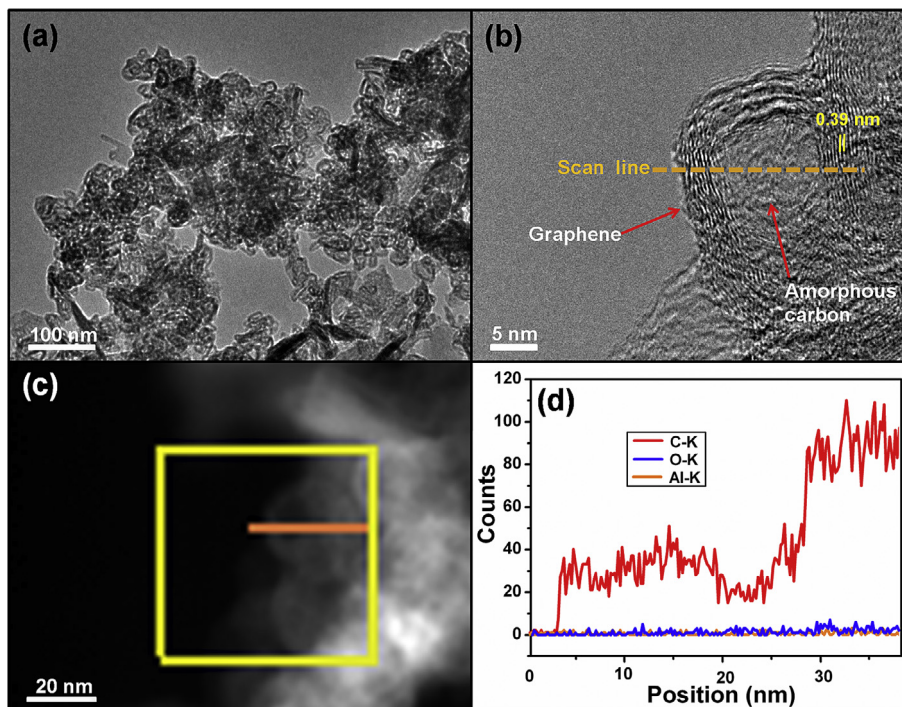


**Fig. 4.** (a) TEM images of the tribofilm debris. The graphene layered nanoscroll structures were observed on HRTEM bright field images (b) and dark field images (c), insert is the line scan range (the scanning direction is from left to right). (d) Line scanning of C, O, Al atoms. (A colour version of this figure can be viewed online.)

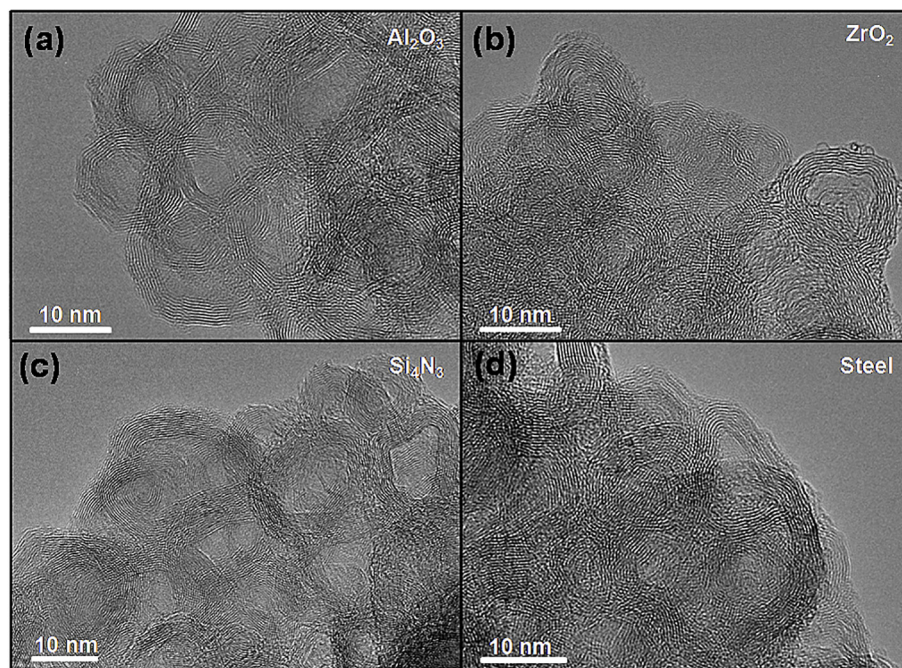


**Fig. 5.** HRTEM images of the tribofilm debris under different duality at 10N, 10 Hz.

amorphous core, initiating the core shell particles formation [29,30]; 3) the sliding graphene patches onto the amorphous core to form GNSs to lowering the energy of the system [29]. This growth mechanism can be surmised from the HRTEM images of tribofilm debris, graphene layers (soft) are easy to package amorphous cores (hard), similar to nanoscroll formation from graphene-plus-nanodiamonds [29]. Fig. 8 gives the growth model for GNS

and friction mechanism transformation of a-C materials. In the initial stage of friction, the non-equilibrium state carbon atoms (Fig. 8a) on the counterparts surface reconfigure under the action of shear stress and friction heat, and transform into graphene (Fig. 8b). Fig. 8b shows the graphene with different layers. Due to the spontaneous reduction of surface energy, the graphene sheets tend to wrap around the amorphous carbon or smaller GNS to

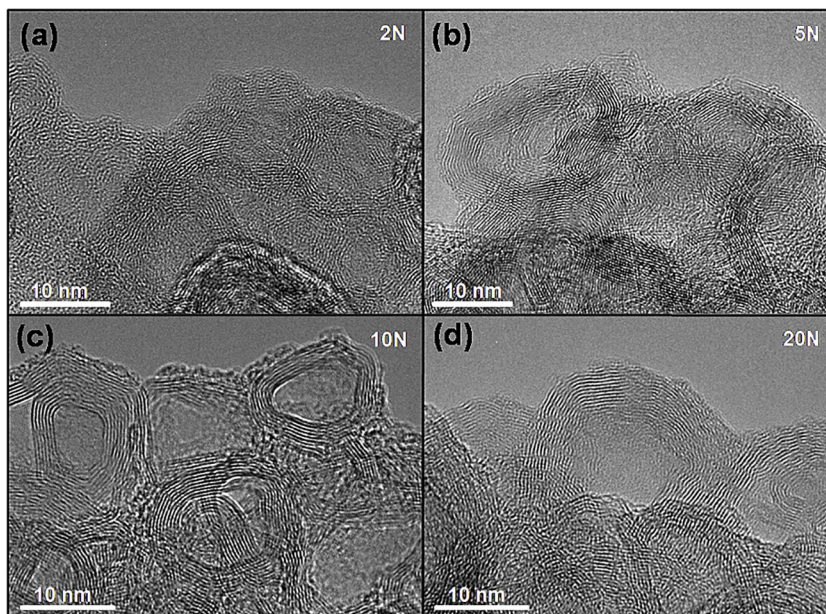


Fig. 6. HRTEM images of the tribofilm debris from  $Al_2O_3$  under different load at 2N, 5N, 10N and 20N, respectively.

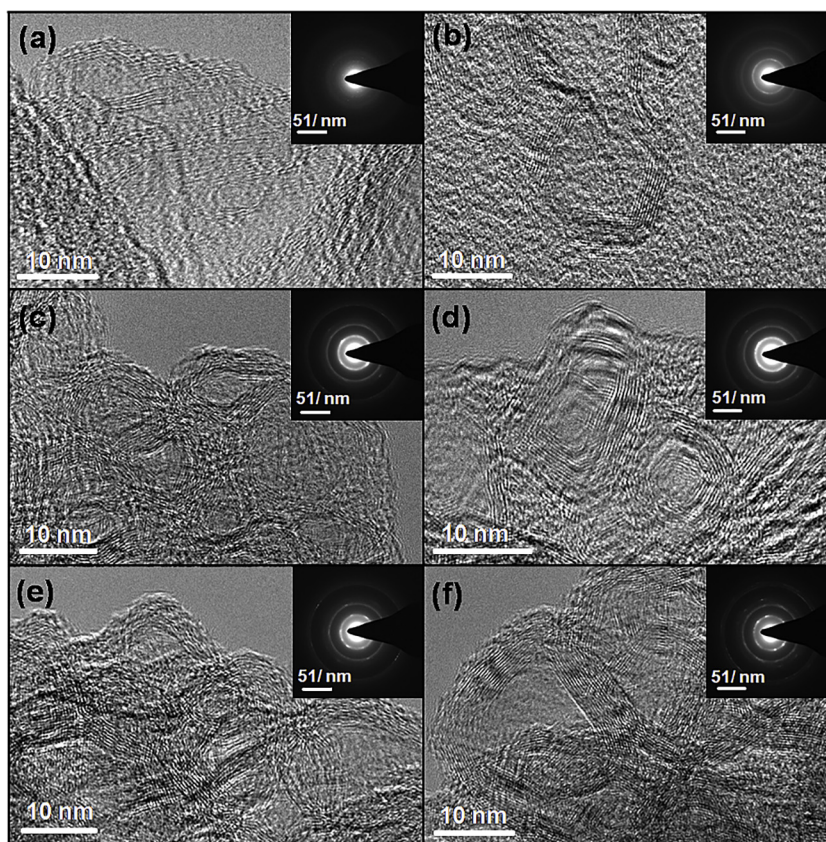
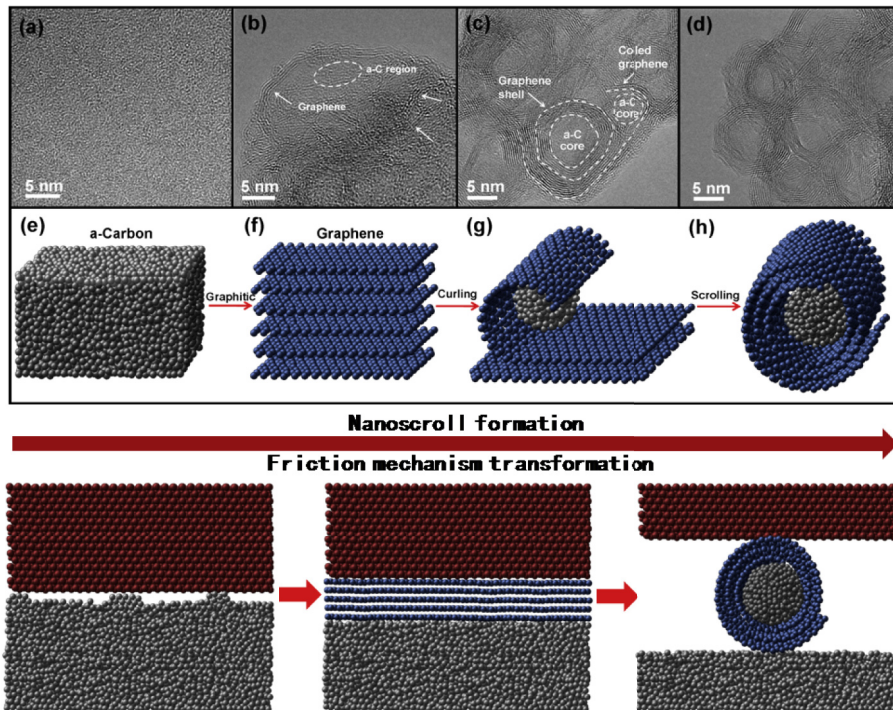


Fig. 7. HRTEM images of the tribofilms fragments: a, b, c, d, e and f at 100, 200, 500, 1000, 2500, 7500 friction cycles, respectively. Insert pictures are the selected area electron diffraction of corresponding debris. Bottom table shows the corresponding friction coefficient at different friction cycles.

**Table 2**  
Corresponding friction coefficient at different friction cycles.

Sliding cycles	100	200	500	1000	2500	7500
Corresponding F.C.	0.068	0.056	0.038	0.022	0.016	0.015

reduce the surface area (Fig. 8c). When the friction process tends to reach an equilibrium state, under the action of shear stress, the bonding recombination occurs at the interface, and finally leads to the formation of large class of GNSs (Fig. 8d). With the aggregation



**Fig. 8.** (a) HRTEM images of original films. (b), (c) and (d) tribofilm debris of 200, 1000 and 7500 friction cycles, at 10N, 10 Hz. (e), (f), (g), (h), Schematic diagram of nucleation and growth model for GNSs. The bottom sketch map show the transformation of friction mechanism of friction interface. (A colour version of this figure can be viewed online.)

of the GNSs, the friction coefficient decreased accordingly. Therefore, this phenomenon herald new friction mechanicals for the super-low friction of a-C films.

Similar to the GNSs, nano-objects, such as carbon onions (COs) and carbon nanotubes (CNTs) show excellent properties in friction and wear reduction [31–36]. The lower friction of these nano spherical particles can be explained by three mechanisms: rolling, sliding and exfoliation [32]. The rolling effect—GNSs acts as a ball bearing between contact surfaces [33–35]. Theoretical modeling predicts that geometrically perfect multi-walled carbon nanotubes (MWNT) would be the “smoothest bearings” [36], with a coefficients of rolling friction generally  $10^2$  to  $10^3$  times lower than sliding friction for corresponding materials [37]. Sliding—the GNSs acts as a separator providing low surface energy of its anisotropy basal plane, resulting low friction and facile shearing mating interfaces due to the incommensurate contact, similarly to superlubricity in graphite [38,39]. Exfoliation—exfoliated layers from the GNSs are deposited on the asperities of the mating surfaces to form a graphitic layer with weak interlayer binding allowing easy shearing [9]. Three main mechanisms could lead to reduced friction and wear of GNSs. Recently, an ultra low macroscopic friction (0.004) is realized by nano scroll formed by graphene-plus-nanodiamonds. Once formed, the atoms of GNSs slide against randomly arranged a-C atoms which provide an incommensurate contact. Moreover, the scrolling induced reduction in nanoscopic contact led to superlow friction state [31]. Molecular dynamics (MD) simulations also suggested that the scroll formation directly contributed to the evolution of the friction coefficient, and the final macro friction coefficient depends on the content of GNSs [31].

From the above discussion, we speculate that the super-low friction of amorphous carbon film originated from the incommensurate contact of GNSs. The GNSs between counter surfaces, which allowed the dual surfaces slide on top of the underlying graphene sheets by overcoming relatively small friction resistance. At the same time, the friction may further reduced by the possible

rolling effect. Therefore, the superlow friction of amorphous carbon film can be surmised from the running-in process. The descent pattern of friction coefficient can be expressed as three stages: 1) initially, surface contamination result in a high friction coefficient. 2) secondly, the formation of graphene sheets creates the lamellar slip mechanism, which reduced the friction coefficient. 3) subsequently, the formation of a large number of GNSs triggers the incommensurate and rolling mechanism, leading to the friction coefficient decreased further.

#### 4. Conclusions

In summary, the friction drop and structural evolution of tribofilm were studied in detail. We firstly found that unique graphene nanoscroll particles were formed in tribofilms. At the same time, the structural evolution of such nano-particles directly contributes to the decrease of macro friction coefficient, independent of the friction test parameter and counterparts. The formation mechanism of such GNSs can be divided into three mechanisms: 1) periodic shear stress leads to the formation of graphene sheets; 2) graphene sheets are highly reactive and easily attach to the dangling bonds on the surface of amorphous core, initiating the core shell particles formation; 3) the sliding graphene patches encounter the 3-D structure of amorphous core. The incommensurate contact between friction surfaces and the graphene scrolls allows dual surface to slide on top of the underlying graphene sheets by overcoming relatively small energetic barriers. Thus, the growth of such nano scroll indicates that incommensurate and rolling contact of GNSs may be the dominant dissipation modes for amorphous carbon.

#### Acknowledgement

The authors are grateful to the National Key Basic Research and Development (973) Program of China (Grant No. 2013CB632304)

and the National Natural Science Foundation of China (51475447, 51611530704 and 51661135022) The authors also thank Lijun Xu for HRTEM and Raman assistance.

## References

- [1] C. Donnet, A. Erdemir, *Tribology of Diamond-like Carbon Films: Fundamentals and Applications*, Springer Science & Business Media, 2007.
- [2] A.H. Lettington, Applications of diamond-like carbon thin films, *Carbon* 36 (5–6) (1998) 555–560.
- [3] K.D. Koshigan, F. Mangolini, J.B. McClimon, B. Vacher, S. Bec, R.W. Carpick, J. Fontaine, Understanding the hydrogen and oxygen gas pressure dependence of the tribological properties of silicon oxide-doped hydrogenated amorphous carbon coatings, *Carbon* 93 (2015) 851–860.
- [4] A.A. Al-Azizi, O. Eryilmaz, A. Erdemir, S.H. Kim, Surface structure of hydrogenated diamond-like carbon: origin of run-in behavior prior to superlubricious interfacial shear, *Langmuir* 31 (5) (2015) 1711–1721.
- [5] I.L. Singer, Mechanics and chemistry of solids in sliding contact, *Langmuir* 12 (19) (1996) 4486–4491.
- [6] L. Pastewka, S. Moser, M. Moseler, Atomistic insights into the running-in, lubrication, and failure of hydrogenated diamond-like carbon coatings, *Tribol. Lett.* 39 (1) (2010) 49–61.
- [7] Y. Liu, A. Erdemir, E.I. Meletis, An investigation of the relationship between graphitization and frictional behavior of DLC coatings, *Surf. Coat. Technol.* 86 (1996) 564–568.
- [8] T.B. Ma, Y.Z. Hu, H. Wang, Molecular dynamics simulation of shear-induced graphitization of amorphous carbon films, *Carbon* 47 (8) (2009) 1953–1957.
- [9] T.B. Ma, L.F. Wang, Y.Z. Hu, X. Li, H. Wang, A shear localization mechanism for lubricity of amorphous carbon materials, *Sci. Rep.* 4 (2014) 3662.
- [10] E. Koren, E. Lörtscher, C. Rawlings, A.W. Knoll, U. Duerig, Adhesion and friction in mesoscopic graphite contacts, *Science* 348 (6235) (2015) 679–683.
- [11] M. Dienwiebel, G.S. Verhoeven, N. Pradeep, J.W. Frenken, J.A. Heimberg, H.W. Zandbergen, Superlubricity of graphite, *Phys. Rev. Lett.* 92 (12) (2004) 126101.
- [12] J. Yang, Z. Liu, F. Grey, Z. Xu, X. Li, Y. Liu, Q. Zheng, Observation of high-speed microscale superlubricity in graphite, *Phys. Rev. Lett.* 110 (25) (2013) 255504.
- [13] H. Zaidi, H. Nery, D. Paulmier, Stability of lubricating properties of graphite by orientation of the crystallites in the presence of water-vapor, *Appl. Surf. Sci.* 70–1 (1993) 180–185.
- [14] A. Grill, Review of the tribology of diamond-like carbon, *Wear* 168 (1–2) (1993) 143–153.
- [15] O.L. Eryilmaz, A. Erdemir, Investigation of initial and steady-state sliding behavior of a nearly frictionless carbon film by imaging 2- and 3-D TOF-SIMS, *Tribol. Lett.* 28 (3) (2007) 241–249.
- [16] I.L. Singer, *Solid Lubrication Processes. Fundamentals of Friction: Macroscopic and Microscopic Processes*, Springer, Netherlands, 1992.
- [17] D.D. Kulkarni, K. Rykaczewski, S. Singamaneni, S. Kim, A.G. Fedorov, V.V. Tsukruk, Thermally induced transformations of amorphous carbon nanostructures fabricated by electron beam induced deposition, *ACS Appl. Mater. Interfaces* 3 (3) (2011) 710–720.
- [18] J.C. Lascovich, R. Giorgi, S. Scaglione, Evaluation of the  $sp^2/sp^3$  ratio in amorphous-carbon structure by XPS and XAES, *Appl. Surf. Sci.* 47 (1) (1991) 17–21.
- [19] L. Pastewka, M. Moseler, The running-in of hydrogenated diamond-like carbon coatings, in: *Proceedings: 25 Years HLRZ/NIC, 7-8 February 2012, Jülich, Germany*, vol. 2012, 2012, 45 215.
- [20] A. Kaniyoor, S. Ramaprabhu, A Raman spectroscopic investigation of graphite oxide derived graphene, *Aip Adv.* 2 (3) (2012) 032183.
- [21] E.H.M. Ferreira, M.V.O. Moutinho, F. Stavale, M.M. Lucchese, R.B. Capaz, C.A. Achete, A. Jorio, Evolution of the Raman spectra from single-, few-, and many-layer graphene with increasing disorder, *Phys. Rev. B* 82 (12) (2010).
- [22] M.A. Tamor, W.C. Vassell, Raman fingerprinting of amorphous-carbon films, *J. Appl. Phys.* 76 (6) (1994) 3823–3830.
- [23] A.C. Ferrari, J. Robertson, Interpretation of Raman spectra of disordered and amorphous carbon, *Phys. Rev. B* 61 (20) (2000) 14095–14107.
- [24] D.H. Ko, R. Sinclair, In-Situ dynamic high-resolution transmission electron-microscopy - application to Pt/Ga as interfacial reactions, *Ultramicroscopy* 54 (2–4) (1994) 166–178.
- [25] S.F. Braga, V.R. Coluci, S.B. Legoas, R. Giro, D.S. Galvao, R.H. Baughman, Structure and dynamics of carbon nanoscrolls, *Nano Lett.* 4 (5) (2004) 881–884.
- [26] G. Carotenuto, A. Longo, S. De Nicola, C. Camerlingo, L. Nicolais, A simple mechanical technique to obtain carbon nanoscrolls from graphite nanoplatelets, *Nanoscale Res. Lett.* 8 (2013) 1–6.
- [27] D. Xia, Q.Z. Xue, J. Xie, H.J. Chen, C. Lv, F. Besenbacher, M.D. Dong, Fabrication of carbon nanoscrolls from monolayer graphene, *Small* 6 (18) (2010) 2010–2019.
- [28] I.G. Goryacheva, *Contact Mechanics in Tribology*, Springer Science & Business Media, 2013.
- [29] D. Berman, S.A. Deshmukh, S.K.R.S. Sankaranarayanan, A. Erdemir, A.V. Sumant, Macroscale superlubricity enabled by graphene nanoscroll formation, *Science* 348 (6239) (2015) 1118–1122.
- [30] D. Xia, Q. Xue, K. Yan, C. Lv, Diverse nanowires activated self-scrolling of graphene nanoribbons, *Appl. Surf. Sci.* 258 (6) (2012) 1964–1970.
- [31] L. Joly-Pottuz, N. Matsumoto, H. Kinoshita, B. Vacher, M. Belin, G. Montagnac, N. Ohmae, Diamond-derived carbon onions as lubricant additives, *Tribol. Int.* 41 (2) (2008) 69–78.
- [32] O. Tevet, P. Von-Huth, R. Popovitz-Biro, R. Rosentsveig, H.D. Wagner, R. Tenne, Friction mechanism of individual multilayered nanoparticles, *Proc. Natl. Acad. Sci.* 108 (50) (2011) 19901–19906.
- [33] M.R. Falvo, R.M. Taylor, A. Helsen, V. Chi, F.P. Brooks, S. Washburn, R. Superfine, Nanometre-scale rolling and sliding of carbon nanotubes, *Nature* 397 (6716) (1999) 236–238.
- [34] M. Lucas, X.H. Zhang, I. Palaci, C. Klinke, E. Tosatti, E. Riedo, Hindered rolling and friction anisotropy in supported carbon nanotubes, *Nat. Mater.* 8 (11) (2009) 876–881.
- [35] J.F. Wu, W.S. Zhai, G.F. Jie, Preparation and tribological properties of  $WS_2$  nanoparticles modified by trioctylamine, *P I Mech. Eng. J4* (2009) 695–703.
- [36] A.N. Kolmogorov, V.H. Crespi, Smoothest bearings: interlayer sliding in multi-walled carbon nanotubes, *Phys. Rev. Lett.* 85 (22) (2000) 4727–4730.
- [37] O.M. Braun, Simple model of microscopic rolling friction, *Phys. Rev. Lett.* 95 (12) (2005).
- [38] P. Saravanan, R. Selyanchyn, H. Tanaka, D. Darekar, A. Staykov, S. Fujikawa, J. Sugimura, Macroscale superlubricity of multilayer polyethylenimine/graphene oxide coatings in different gas environments, *ACS Appl. Mater. Interfaces* 8 (2016) 27179–27187.
- [39] Z. Liu, J. Yang, F. Grey, J.Z. Liu, Y. Liu, Y. Wang, Q. Zheng, Observation of microscale superlubricity in graphite, *Phys. Rev. Lett.* 108 (20) (2012) 205503.